Digital Signal Processing 40 (2015) 164–175

Contents lists available at ScienceDirect

Digital Signal Processing

www.elsevier.com/locate/dsp

An unconstrained optimization approach to empirical mode decomposition

Marcelo A. Colominas [a,b], Gastón Schlotthauer [a,b,c,*], María E. Torres [a,b]

[a] Laboratorio de Señales y Dinámicas no Lineales, Universidad Nacional de Entre Ríos, Ruta Prov. 11 Km 10.5, Oro Verde, Entre Ríos, Argentina
[b] Consejo Nacional de Investigaciones Científicas y Técnicas (CONICET), Argentina
[c] Centro de Investigaciones y Transferencia de Entre Ríos (CITER) CONICET-UNER, Argentina

ARTICLE INFO

Article history:
Available online 26 February 2015

Keywords:
Empirical mode decomposition (EMD)
Convex optimization
Time frequency
Data-driven methods

ABSTRACT

Empirical mode decomposition (EMD) is an adaptive (data-driven) method to decompose non-linear and non-stationary signals into AM-FM components. Despite its well-known usefulness, one of the major EMD drawbacks is its lack of mathematical foundation, being defined as an algorithm output. In this paper we present an alternative formulation for the EMD method, based on unconstrained optimization. Unlike previous optimization-based efforts, our approach is simple, with an analytic solution, and its algorithm can be easily implemented. By making no explicit use of envelopes to find the local mean, possible inherent problems of the original EMD formulation (such as the under- and overshoot) are avoided. Classical EMD experiments with artificial signals overlapped in both time and frequency are revisited, and comparisons with other optimization-based approaches to EMD are made, showing advantages for our proposal both in recovering known components and computational times. A voice signal is decomposed by our method evidencing some advantages in comparison with traditional EMD and noise-assisted versions. The new method here introduced catches most flavors of the original EMD but with a more solid mathematical framework, which could lead to explore analytical properties of this technique.

1. Introduction

Empirical Mode Decomposition (EMD) [1] is an adaptive method introduced to analyze non-linear and non-stationary signals. It consists in a local and fully data-driven separation of a signal in fast and slow oscillations. At the end of the decomposition, the original signal can be expressed as a sum of amplitude and frequency modulated (AM–FM) functions called *intrinsic mode functions* (IMFs) plus a final trend either monotonic or constant. However, EMD experiences some problems, such as the presence of oscillations of very disparate amplitude in a mode, or the presence of very similar oscillations in different modes, named as *mode mixing* (an interesting strategy to alleviate noise-related mode mixing can be found in [2]). Besides this issue, one of its major drawbacks is the lack of mathematical framework, being defined as an algorithm output.

Several efforts have been made in order to provide some mathematical foundations for EMD. Deléchelle et al. [3] estimated the envelopes by solving a parabolic differential equation. Xu et al. [4] modified the envelope definition to obtain one with a simple analytical expression, by which the variations of the extrema in the iterative procedure are investigated in detail to reveal the nature of the sifting process. Hawley et al. [5] replaced the cubic spline interpolations for trigonometric interpolations when estimating the envelopes. Thanks to that, they derive some interesting properties and convergence guarantees, although the results significantly differ from those of classical EMD. Daubechies et al. [6,7] compared EMD with wavelet theory by using a special case of reassignment called *synchrosqueezing*.

A different approach, based on optimization theory, has recently aroused the interest of the EMD scientific community. B. Huang and Kunoth [8] replaced the explicit interpolation through extrema for solving an optimization problem to estimate the envelopes. However, they keep an envelope-related approach. No explicit envelope is estimated by Oberlin et al. in [9]. They search for a local mean in a specific B-spline space subject to some symmetry constraints on the amplitude of the modes. In a similar way, Pustelnik et al. [10,11] minimized the difference between a signal and its local mean plus mode subject to smoothness, symmetry

* Corresponding author at: Universidad Nacional de Entre Ríos, Laboratorio de Señales y Dinámicas no Lineales, Ruta Prov. 11 Km 10.5, 3100, Oro Verde, Entre Rios, Argentina.
E-mail addresses: macolominas@bioingenieria.edu.ar (M.A. Colominas), gschlotthauer@conicet.gov.ar (G. Schlotthauer), metorres@santafe-conicet.gov.ar (M.E. Torres).

http://dx.doi.org/10.1016/j.dsp.2015.02.013
1051-2004/

and quasiorthogonality requirements, based on a multicomponent variational analysis.

In this paper, we propose a new approach for EMD based on optimization, with the goal of mimic EMD. Unlike those above mentioned, here we present an unconstrained optimization problem, with a unique analytic solution. This results in the following benefits:

- This approach may help to better understand some properties of EMD.
- The explicit computation of envelopes to find the local mean is not needed, in contrast to algorithm-based EMD.
- The proposed method provides an analytical and easily implemented closed solution, unlike previous optimization-based efforts that need iterative algorithms to solve the optimization problem.
- The use of explicit spline interpolations is avoided.
- The number of parameters to be tuned has been reduced to only one, in contrast to other optimization-based proposals where several parameters are needed.
- The computational cost is similar to the cost of EMD. On the contrary, other optimization-based methods are tens of times slower than EMD.

The paper is organized as follows. We recall the basic principles of EMD in Section 2. In Section 3 we present our new unconstrained optimization approach to EMD. Experiments and results with both artificial and real signals are introduced and discussed in Section 5. Conclusions are presented in Section 6.

2. Empirical mode decomposition

The main idea on EMD is to iteratively subtract the local mean from a signal (or residue) to obtain the zero local mean AM–FM components called intrinsic mode functions or simply modes. From this perspective, the slow oscillation is considered the local mean (trend) while the mode is the fast one. If x is the signal to be decomposed, the EMD algorithm can be summarized as follows [1]:

1. Set $k=0$ and find all extrema of $r_0=x$.
2. Interpolate between minima (maxima) of r_k to obtain the lower (upper) envelope e_{min} (e_{max}).
3. Compute the mean envelope $m=(e_{min}+e_{max})/2$.
4. Compute the IMF candidate $d_{k+1}=r_k-m$.
5. Is d_{k+1} an IMF?
   - Yes. Save d_{k+1}, compute the residue $r_{k+1}=x-\sum_{i=1}^{k+1} d_i$, $k=k+1$, and treat r_k as input data in step 2.
   - No. Treat d_{k+1} as input data in step 2.
6. Continue until the final residue r_K satisfies some predefined stopping criterion.

At the end, the signal x can be expressed as

$$x=\sum_{i=1}^{K} d_k + r_K, \tag{1}$$

where each mode d_k admits well-behaved Hilbert transforms. The refinement process carried out to ensure that the mode d_k is actually an IMF is the so-called *sifting process*. Further details can be found in [1].

The symmetry of the modes' envelopes resides on the IMF definition. To be considered an IMF, a function must fulfill two conditions: (i) the number of extrema and zero crossings are equal or differ at most by one; and (ii) the mean between the upper and lower envelope is zero for all the signal duration.

Some of the main characteristics of the EMD are its multiscale and local nature. The local scale is defined as the interval between successive extrema. The number of extrema of the modes decreases as k increases. Although one may give "spectral" interpretation of the modes, it must be emphasized that this applies only locally. The automatic selection of the local highest frequency content cannot be achieved by a predetermined subband filtering; it rather corresponds to an adaptive (data-dependent) time-variant filtering [12]. When decomposing fractional Gaussian noise (fGn), EMD acts on average as a dyadic filter bank [12,13].

3. EMD as an unconstrained non-linear convex optimization problem

Notice that, in the original EMD algorithm, the local mean is defined as the mean of the envelopes, which are obtained by interpolating through local extrema (usually with cubic splines). Therefore, from the second mode onwards, all of them are sums of splines. We must get rid of the envelopes, so we propose here a different approach to obtain the local mean. Previous efforts have focused their attention on the smoothness of the local mean [14] (even restricting their search to a spline subspace [9]). In those approaches, the IMF-likeness of the modes is not considered on the objective function but in the form of inequality constraints, where the corresponding bounds have to be set. However, the IMF conditions are the heart of EMD and the sifting process is carried out until the mode is close enough to an IMF, so the original signal is the sum of IMFs plus a final trend. For this reason, our proposal focuses on the IMF-likeness of the modes.

Let us return to the IMF definition in Section 2. It is clear that condition (ii) cannot be satisfied without fulfilling condition (i), so it is enough to pursuit condition (ii). We consider this issue in a similar fashion to Oberlin et al. [9] and Pustelnik et al. [10]. Let $t_k[l]$, $1\le l\le L$, with L the number of local extrema, be the locations of the local extrema of the signal (or residue) under study. If we consider these points as estimations of the local extrema locations of the k-th mode (d_k), for $2\le l\le L-1$, we can define the inner product

$$p^k_{t_k[l]}\, d_k = d_k(t_k[l]) + \frac{d_k(t_k[l+1])\Delta_l^- + d_k(t_k[l-1])\Delta_l^+}{\Delta_l^+ + \Delta_l^-}, \tag{2}$$

where $\Delta_l^+ = t_k[l+1]-t_k[l]$, $\Delta_l^- = t_k[l]-t_k[l-1]$, d_k is a column vector and $p^k_{t_k[l]}$ is the $t_k[l]$-th row of a matrix P^k. Then, the only non-zero elements of the $t_k[l]$-th row of P^k are

$$P^k(t_k[l], t_k[l]) = 1, \tag{3a}$$

$$P^k(t_k[l], t_k[l-1]) = \frac{\Delta_l^+}{\Delta_l^+ + \Delta_l^-}, \tag{3b}$$

$$P^k(t_k[l], t_k[l+1]) = \frac{\Delta_l^-}{\Delta_l^+ + \Delta_l^-}. \tag{3c}$$

It should be emphasized the fact that matrix P^k has as many rows as the length of d_k. Rows not involved in (2) are zeros, because there are no local extrema at that positions. The goal of (2) is to compare the signal (or residue) at each extrema with the corresponding linear interpolation between its two adjacent extrema. Smaller values of (2) would mean that d_k locally (around $t_k[l]$) better satisfies the IMF condition (ii). The minimization of $||P^k d_k||^2$ would contribute, at least globally, to the fulfillment of the IMF conditions. As it was pointed out by Pustelnik et al., matrix P is a *"...linear operator which models the penalization imposed on d at each location $t_k[l]$"* [10]. It must be noticed that, in this approach, the IMF conditions are not evaluated over the whole time span of the signal but only on its local extrema.

Given a signal x, we can define our quest for a first mode by searching for a local mean (or approximation) a which minimizes $||P^1(x-a)||^2$. A solution to this problem is $x=a$, of course undesirable. However, this solution is not unique since P may be singular. Because of that, we must regularize our problem. To favor smooth solutions, we choose a second-order Tikhonov regularization [15]. With this in mind, we can formulate the following optimization problem:

$$\text{(P)} \qquad \min_a \underbrace{||P(x-a)||^2 + \lambda||Da||^2}_{f(a)},$$

with its unique solution at

$$\begin{aligned} \nabla_a f = -2P^TP(x-a) + 2\lambda D^TDa = 0 \Rightarrow \\ \Rightarrow P^TPa + \lambda D^TDa = P^TPx \\ a^* = (P^TP + \lambda D^TD)^{-1}P^TPx, \end{aligned} \quad (4)$$

where x is the signal, a the estimated local mean, D the second-order difference matrix, $||\cdot||$ is the Euclidean norm and $\lambda > 0$ the regularization parameter used to control the trade-off between the smoothness of a and the IMF-likeness of the mode $d = x - a$.

Using problem (P) and its closed solution given by (4) we can formulate the following algorithm:

Algorithm 1

1: Choose $\lambda > 0$.
2: Define the second-order difference matrix

$$D = \begin{bmatrix} -2 & 1 & & & \\ 1 & -2 & 1 & & \\ & \ddots & \ddots & \ddots & \\ & & 1 & -2 & 1 \\ & & & 1 & -2 \end{bmatrix}.$$

3: Assign $a_0 = x$ (signal).
4: **for** $k = 1, 2, \ldots$ **do**
5: Construct the matrix P^k, according to (2), by using the local extrema from a_{k-1}.
6: Calculate the local mean a_k

$$M_1 = (P^k)^T P^k + \lambda D^T D \quad (5a)$$

$$M_2 = (P^k)^T P^k \quad (5b)$$

$$a_k = M_1^{-1} M_2 a_{k-1} \quad (5c)$$

7: Calculate the mode $d_k = a_{k-1} - a_k$.
8: **end for**

In the above algorithm we perform only one "sifting" iteration (steps 5 to 7 for a fixed k) for each mode extraction. However, it is possible to use more iterations.

Matrix P^k makes this method adaptive (data-driven) and local, with local extrema as characteristic points. A comment regarding the regularization parameter must be done. As λ tends to infinity, the approximation a becomes affine. However, according to our studies, the here presented method behaves robust to the choice of λ. In order to study its influence, in our first experiment, in Section 5.1, we will explore different values for this parameter. Thereafter, despite being in very different situations, we will always use the same value $\lambda = 1$. Objective methods to choose the regularization parameter, such as the L-curve method or Morozov's discrepancy principle could be employed, but such options involve an expensive computational cost.

Regularization process is crucial for the problem to be solvable. Since matrix P (we drop the index k for the sake of simplicity) may be not invertible, as it occurs in most cases, it is essential to add the penalization term to the optimization problem. Because of that, a unique solution is achieved since symmetric matrix $P^TP + \lambda D^TD$ is positive definite:

$$\begin{aligned} y^T(P^TP + \lambda D^TD)y &= y^TP^TPy + \lambda y^TD^TDy \\ &= (Py)^TPy + \lambda(Dy)^TDy > 0, \forall y \neq 0, \end{aligned} \quad (6)$$

due to $\mathcal{N}(P) \cap \mathcal{N}(D) = \{0\}$: $Dy = 0$ only for linear functions y, for which P is null (no local extrema) and it would make no sense to even formulate problem (P). Therefore it is only necessary for λ to be positive. However, a very small value of λ (i.e., $\lambda \to 0$) will lead to a large condition number, and results might be inaccurate.

In order to efficiently solve the matrix inversion involved in (5c), we must explore the particular structure of matrix M_1. For a signal of length N, matrix D^TD has $5N-6$ nonzero elements and matrix P^TP has $5L$ entries which are nonzero, but L of those elements are on the main diagonal. Then, the nonzero elements of matrix $P^TP + \lambda D^TD$ are

$$5N - 6 + 4L \leq 9N - 6 < 9N, \quad (7)$$

hence the proportion of nonzero elements is bounded by $9/N$, which means that this matrix is sparse. Another important feature for this matrix is being band diagonal, with a matrix bandwidth of $bw = \max_l(t[l] - t[l+2])$ [16]. Sparsity of matrices P and D is exploited in the implementation and a significant amount of computational time is saved.

Let us take a deeper look at (5). Since symmetric matrix $M_2 = (P^k)^TP^k$ has non-zero columns only on the extrema locations ($t_k[l]$-th columns), the product $\Phi = M_1^{-1}M_2$ has exactly L non-zero columns. Because of that, we can write

$$a_k = \Phi\, a_{k-1} = \sum_{l=1}^{L} \phi_{t_k[l]}\, a_{k-1}(t_k[l]), \quad (8)$$

where $\phi_{t_k[l]}$ stands for the $t_k[l]$-th column of Φ and $a_{k-1}(t_k[l])$ is the signal (or residue) evaluated at its local extrema. Therefore, the local mean a_k is in the subspace created by the non-zero columns of Φ, and the values of the signal at its local extrema are the coefficients. This "sparse" representation of a_k is consistent with the original formulation for EMD, where the local mean only depends on the locations of the local extrema and the values of the signal at those points.

Every method that uses local extrema of the signal to estimate those of the extracted component may need some form of sifting. If some of the mode extrema are hidden (they do not appear in the composed signal), these can be revealed after one round of sifting [17,18]. Then, the proto-IMF would have more extrema than the original signal, and matrix P (constructed from the extrema of the original signal) would not be able to model the penalization on it. A new matrix P would need to be constructed, and a new trend extraction would be performed. In our particular case, sifting may also help the method to work properly.

Two different strategies for stopping the sifting process (steps 5 to 7 for a fixed k) will be used in this work. Such as in traditional EMD, one may use a fixed number of sifting iterations [19,20]. However, it may be also interesting to use a variable number of iterations, especially for real signals. Then, an *objective* stopping criterion is needed. Since no envelope is computed, it is not possible to apply a local/global criterion, like the one proposed in [21], to check IMF condition (ii). Nevertheless, an energy-based criterion could be used to decide whether or not the mode d_k has zero mean. In those cases, following [20], we use

$$z = \frac{||\hat{a}_k^{(i+1)}||^2}{||d_k^{(i)}||^2}, \quad (9)$$

where $\hat{a}_k^{(i+1)}$ stands for the local mean computed from the i-th candidate for the k-th mode $d_k^{(i)}$ (the proto-IMF after i iterations of sifting), with the recommended value of $z = 10^{-4}$ [20]. A Matlab toolbox for the proposed method is available on our website (www.bioingenieria.edu.ar/grupos/ldnlys).

We will call our method UOA-EMD in what follows.

4. Related works

4.1. Optimization-based approaches to EMD

One of the first efforts in explaining EMD through optimization techniques is due to Meignen and Perrier [14]. This work was extended by Oberlin et al. in [9]. They found the local mean of a signal by solving the following problem:

$$\text{(P2)} \qquad \min_{a} ||a^{(2)}||^2 \text{ s. t. } a \in \Pi \cap C_{a_{k-1}},$$

where Π denotes the space of spline functions and $C_{a_{k-1}}$ denotes a constraint which imposes the symmetry of envelopes. Besides not having an analytical closed solution, the main drawback of this proposal is that it requires a first approximation $\bar{a}$ as a primer to the algorithm in order to involve a convex constraint. This approximation $\bar{a}$ is found *via* explicit spline interpolation following the proposal in [22], which presents some problems in the presence of strong FM signals. It also needs two parameters to be set: the order of the spline space of functions and a tolerance α for the symmetry of the modes. The authors recommend an order of 6 or higher for the spline space and $\alpha = 0.05$ for the tolerance. An implementation of this method is available at http://www-ljk.imag.fr/membres/Thomas.Oberlin/EMDOS.tar.gz. It will be named as OS-EMD, for optimization on splines, in what follows.

A multicomponent non-smooth convex optimization approach to EMD was introduced by Pustelnik et al. in [10], and it was more deeply explained in [11]. The optimization problem to be solved is the following:

$$\text{(P3)} \quad \min_{a,d} ||a_{k-1} - a - d||^2, \text{s.t.} \begin{cases} ||Da||_p^p \le \eta_k, \\ ||P^k d||_q^q \le \varepsilon_k, \\ (\forall j < k), |\langle d, d_j \rangle| \le \zeta_{k,j}, \end{cases}$$

where $\eta_k > 0$, $\varepsilon_k > 0$, $\zeta_{k,j} \ge 0$, $p \ge 1$, $q \ge 1$ and D is the first or second order derivative operator. Several parameters need to be set for this method: the bounds η_k, ε_k, and $\zeta_{k,j}$, along with the norms p and q and the order of the derivative (matrix D). It must be noticed that this method does not guarantee the exact reconstruction of the data, since $||a_{k-1} - a - d||^2$ must be minimized but is not exactly zero. An implementation of this method is available at http://perso.ens-lyon.fr/nelly.pustelnik/Software/Prox-EMD_v1.0.zip. Rather than solving the above described problem, the toolbox solves the following one: $\min_{a,d} ||a_{k-1} - a - d||_p^p + c_1||Da||_q^q + c_2||P^k d||_r^r$. They replaced the constrained problem for the regularized version and dropped the quasiorthogonality constraints. Because of that, it is not possible to reproduce the simulations from [10,11] since the parameters they reported were for the constrained problem. The default setting is: $p = 2$, $q = 2$, $r = 1$ and second order for the derivative. (Please notice that the norms p, q and r of the toolbox differ from the norms p and q of the original problem (P3).) In this case, the number of modes and values c_1 and c_2 are determined from the classical EMD decomposition of the data. This proposal will be named as Prox-EMD in what follows.

4.2. Other mode decomposition proposals

Peng and Hwang [23] proposed an adaptive operator-based signal separation method, where they introduced an equation of the same form as in (4), and the obtained components are in the null space of such operator (which plays the role of matrix P in our approach). Although they proposed two options for the operator (an integral operator and a differential one), some particular signals cannot be correctly separated into their components by this method, as the authors themselves have pointed out. We will see in Section 5.4 that the method here proposed is able to correctly decompose such signals.

The work from [23] was expanded by the same authors in [24]. Although this approach was an improvement, it is also much more complicated, involving an objective function with several terms. Also some parameters need to be carefully tuned. However, the main differences are the final goals of the methods. The proposals in [23,24] do not intend to emulate EMD, and because of that their operators do not take into account the specific IMF features. In contrast, in our approach operator P is constructed with EMD-inspired features such as the symmetry of the modes. The proposal in [24] do not take into account a fine to coarse nature for their decomposition, and thus their goal significantly differs from that of EMD's. Recursive algorithms are needed to solve it, with no analytical solution available.

5. Experiments and results

In order to better understand the capabilities of the new approach introduced in this paper, in this section we revisit some classical experiments with artificial signals and compare our results with those obtained *via* traditional EMD. In addition, we present an experiment with real data comparing our results with traditional EMD and noise-assisted versions such as Ensemble EMD (EEMD) [20] and Complete EEMD with Adaptive Noise (CEEMDAN) [25,26].

5.1. One or two frequencies?

As first experiment we revisit the pioneer work by Rilling and Flandrin [17]. Let us define a sum of two tones

$$x(t; \alpha, f) = s_1 + s_2 = \sin(2\pi t) + \alpha \sin(2\pi f t) \tag{10}$$

with $f \in (0, 1)$ and $\alpha > 0$. Although simple, this model proved to be very effective in evaluating EMD performance. Our goal is to deduce (and then to measure) the performance of our method when applied to x. The fine to coarse nature of our proposal suggests that the first mode d_1 must catch most of s_1 (the fastest tone). We are interested in answering the following question: under what conditions is $d_1 \approx s_1$?

From Algorithm 1, we can see that $d_1 \approx s_1$ is equivalent to $a_1 \approx s_2$. If we apply (5c) to our signal x, we get

$$a_1 = M_1^{-1} M_2 x = M_1^{-1} M_2 s_1 + M_1^{-1} M_2 s_2, \tag{11}$$

with M_1, M_2 depending on P^1, which is obtained from the extrema of x. It becomes clear that a sufficient condition to separate the two tones (i.e. to get $a_1 \approx s_2$) is

$$M_1^{-1} M_2 s_1 = \left((P^1)^T P^1 + \lambda D^T D\right)^{-1} (P^1)^T P^1 s_1 \approx 0 \tag{12}$$

and

$$\begin{aligned} M_1^{-1} M_2 s_2 &= \left((P^1)^T P^1 + \lambda D^T D\right)^{-1} (P^1)^T P^1 s_2 \\ &= \left((P^1)^T P^1 + \lambda D^T D\right)^{-1} \left((P^1)^T P^1 + \lambda D^T D - \lambda D^T D\right) s_2 \\ &= \left(I - \left((P^1)^T P^1 + \lambda D^T D\right)^{-1} \lambda D^T D\right) s_2 \\ &= s_2 - \left((P^1)^T P^1 + \lambda D^T D\right)^{-1} \lambda D^T D s_2 \approx s_2. \end{aligned} \tag{13}$$

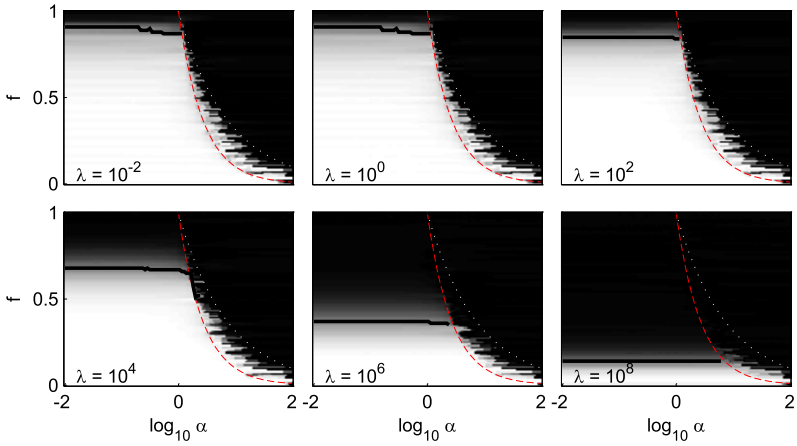

Fig. 1. Separation of a sum of two tones. Criterion (14) is plotted in a 2-D image. Critical curves are superimposed as red [gray] dashed ($\alpha f = 1$) and white dotted ($\alpha f^2 = 1$). The black thick line for $\alpha f < 1$ represents the cut-off frequency for which $c(\alpha, f) = 0.5$. In the images, color white means a value of 0 and color black means 1.

Rilling and Flandrin [17] demonstrated that if the product αf is sufficiently smaller than 1, then the extrema from x are close to those of s_1 and, since s_1 is a pure tone with zero local mean, $P^1 s_1 \approx 0$, satisfying (12). Also αf smaller than 1 ensures that the fourth derivative of s_2 (i.e., $D^T D s_2$) is small, and if λ is small too, (13) is satisfied.

Now we have an answer for the question stated above. For αf small ($\alpha f < 1$ is enough), and λ also small, the separation will be satisfactory and $d_1 \approx s_1$. To measure our method performance, following [17], we propose to compute

$$c(\alpha, f) = \frac{||d_1(t; \alpha, f) - s_1||}{||s_2||}, \tag{14}$$

where $d_1(t; \alpha, f)$ stands for the first mode obtained from $x(t; \alpha, f)$ and $||\cdot||$ the Euclidean norm. A zero value of $c(\alpha, f)$ indicates a correct separation, while a value close to one occurs when the two tones are poorly separated.

Fig. 1 presents the results, with $f \in (0, 1)$ and $10^{-2} \leq \alpha \leq 10^2$, for six values of λ. Signals of 2000 samples with a sampling frequency of 200 Hz were used. The parameter f had 100 bins. The criterion (14) was evaluated over samples 501 to 1500. The resemblance with the results presented in [17] is remarkable. In the top row, two well-separated areas can be identified. For $\alpha f < 1$ the two tones are perfectly separated, except for above a "cut-off" frequency $f_c \approx 0.9$ where it is impossible to separate the two components, no matter the amplitude ratio. This result is consistent with our expectations that the two tones would be correctly separated if αf is small enough. On the other hand, for $\alpha f^2 > 1$, the two tones are badly separated. Rilling and Flandrin [17] showed that, for this domain, the slowest tone is "dominant" with the extreme rate of the signal equal to that of the low frequency one. Therefore, it seems logical that our method (such as traditional EMD) is unable to catch the fastest tone on its first mode if the extrema from this tone are absent from the composed signal. There is a transition zone (sort of a "no-man's land") between the two mentioned domains where the separation performance seems to be mainly conditioned by the frequency ratio f. It is worth of mention that to reach a cut-off frequency $f_c \approx 0.9$ with EMD, it is necessary to perform over 100 sifting iterations [17]. In our case, we used only one iteration, and therefore the stopping criterion (9) was not needed.

In the bottom row of Fig. 1, the results are still similar to the previous ones, but yet quite different. The two areas (and the transition zone) are still recognizable, but the cut-off frequency is smaller as λ increases. These results suggest that λ can be selected from a wide range of values, evidencing the robustness of our method. In what follows, and for the sake of simplicity, we will use $\lambda = 1$, a value for which we got very good results in very different situations, as we will see in the next experiments.

5.2. Composites of AM–FM and non-linear oscillations

The first experiment in this subsection was performed on a signal very similar to one studied in [10]. It consists in a sum of a fast tone and a slow tone of different amplitudes and a Gaussian atom with a middle frequency, containing 1000 datapoints. In Fig. 2 we present the decomposition results obtained traditional EMD, Prox-EMD, OS-EMD and the method here proposed UOA-EMD. In all cases, the number of modes $K = 3$ to decompose was assumed as known. The trade-off parameter for UOA-EMD was $\lambda = 1$, and only one sifting iteration for each component extraction was performed. To compare the results with the original signal components, we used the relative squared error (RSE)

$$RSE_d(\hat{d}) = \frac{||\hat{d} - d||^2}{||d||^2}, \tag{15}$$

where d is a given signal and $\hat{d}$ its estimation. Both Prox-EMD and OS-EMD were used on its default settings. For traditional EMD, we used the toolbox available at http://perso.ens-lyon.fr/patrick.flandrin/emd.html, with the default stopping criterion. Table 1 presents the RSEs and computational times for the four methods. For all three components, the errors for EMD and UOA-EMD are of comparable magnitudes, while those of the other two methods are at least one order of magnitude higher. Computational times also ask for a deeper observation. The time for our method UOA-EMD is six times lower than EMD's, and two orders of magnitude lower than those of the other two methods. (We ran all the simulations on a PC with an Intel(R) Core(TM) i7-4770K CPU @ 3.50 GHz.)

As a second experiment for this subsection, a signal very similar to one studied in [27] was decomposed *via* the four methods. The signal is a sum of three components: a "high frequency" triangular waveform with a slowly linearly increasing amplitude, a "middle frequency" tone with a quickly linearly decreasing amplitude, and a "low frequency" triangular waveform. As before, it consists of 1000 datapoints. Results are depicted in Fig. 3. Again, $\lambda = 1$ was used for UOA-EMD and only one sifting iteration was performed. RSEs and computational times can be appreciated on Table 2. The values resemble those of the previous example. The errors for EMD and UOA-EMD are of comparable magnitude and at least one order of magnitude lower than those of Prox-EMD and OS-EMD (with this difference increased to two order of magnitude for two Prox-EMD

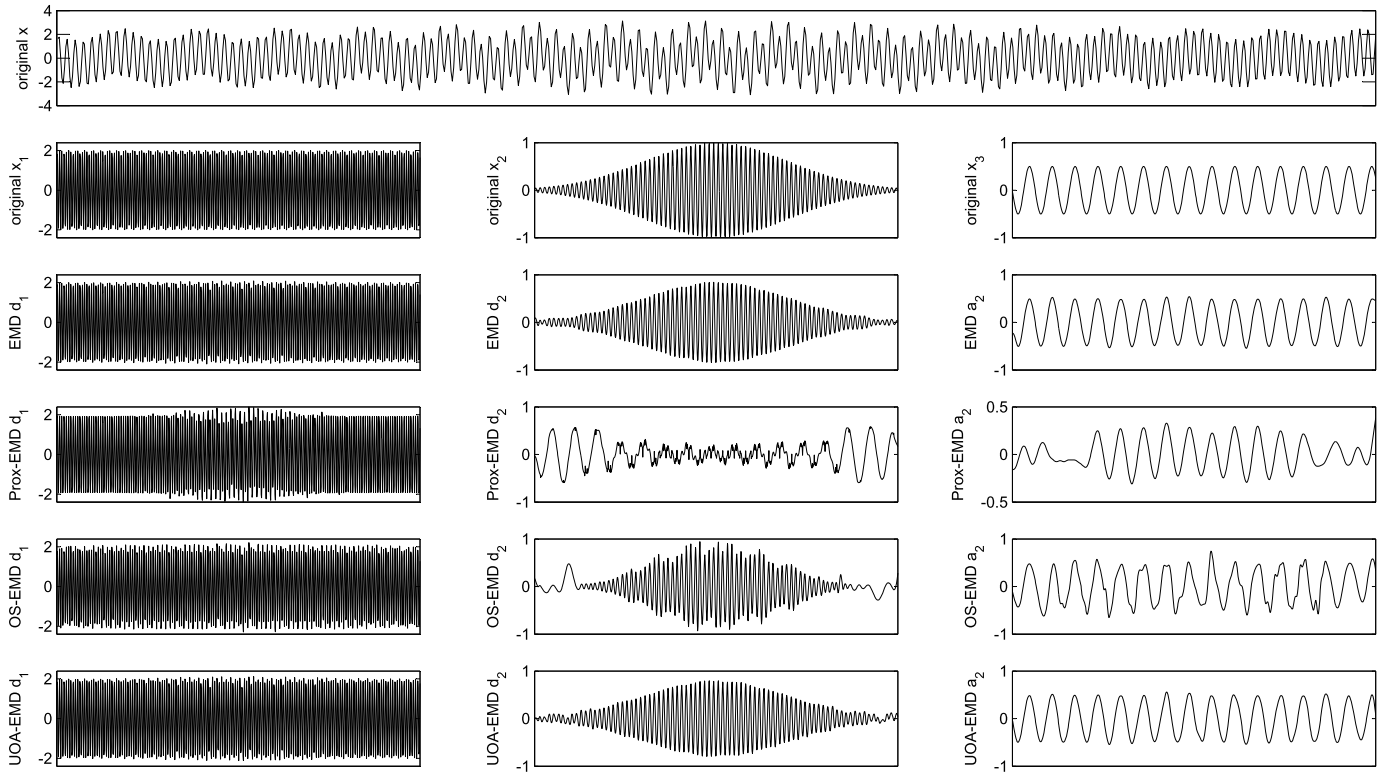

Fig. 2. Sum of two tones and a Gaussian atom. The original signal x is on the top row, and its components are on the second row. On the following rows are the components extracted *via* traditional EMD, Prox-EMD, OS-EMD and UOA-EMD respectively.

Table 1
Sum of two tones and a Gaussian atom (1000 datapoints). Relative square errors and computational times for the four methods.

	Relative square error			Computational time (seconds)
	$x_1(t)$	$x_2(t)$	$x_3(t)$	
EMD	$\mathbf{2.30 \times 10^{-3}}$	$\mathbf{2.42 \times 10^{-2}}$	$\mathbf{3.70 \times 10^{-3}}$	0.0717
Prox-EMD	5.29×10^{-2}	1.1615	5.88×10^{-1}	3.1490
OS-EMD	1.19×10^{-2}	1.59×10^{-1}	9.39×10^{-2}	7.0712
UOA-EMD	4.00×10^{-3}	4.27×10^{-2}	8.30×10^{-3}	**0.0110**

Table 2
Sum of two triangular waveforms and an FM sinusoidal signal (1000 datapoints). Relative square errors and computational times for the four methods.

	Relative square error			Computational time (seconds)
	$x_1(t)$	$x_2(t)$	$x_3(t)$	
EMD	1.50×10^{-2}	8.10×10^{-3}	8.00×10^{-4}	0.0679
Prox-EMD	7.14×10^{-1}	6.2173	2.05×10^{-1}	3.0362
OS-EMD	4.06×10^{-1}	7.366	2.53×10^{-1}	5.4287
UOA-EMD	$\mathbf{1.27 \times 10^{-2}}$	$\mathbf{3.30 \times 10^{-3}}$	$\mathbf{7.00 \times 10^{-4}}$	**0.0104**

components). Computational times are also similar to those of the previous example. UOA-EMD needed a sixth of time of EMD, and two orders of magnitude less than that needed for Prox-EMD and OS-EMD.

As a third and final experiment for this subsection, we analyzed a very similar signal to one used in [21]. It is a sum of two FM sinusoidal signals and a Gaussian atom, all three overlapped both in time and frequency. In order to test our method UOA-EMD for large data, the signal to decompose consists of a million datapoints. The decompositions results can be seen in Fig. 4. As in previous examples, we used $\lambda = 1$ and one sifting iteration. Table 3 presents both the RSEs and computational times. UOA-EMD achieved errors of one order of magnitude lower than EMD for all three components, and at least two orders of magnitude lower than that of Prox-EMD. The method OS-EMD did not accomplished the decomposition, printing an error message after almost 12 minutes of execution. Computational times deserve some comments. EMD needed a little more than one second, while UOA-EMD took almost three seconds. In contrast, Prox-EMD needed more than 47 minutes.

In this subsection we have illustrated with classical artificial signals our method's capabilities, successfully decomposing signals with AM–FM components and non-linear oscillations overlapped in time and frequency. In all cases results are similar to those obtained by EMD. Relative squared errors are of the same magnitude order. The computational cost of our method is similar to EMD's. In contrast, the other two optimization-based methods achieved errors of at least one order of magnitude higher and times of at least two orders of magnitude higher. These differences were dramatically increased when a million-datapoint signal was analyzed.

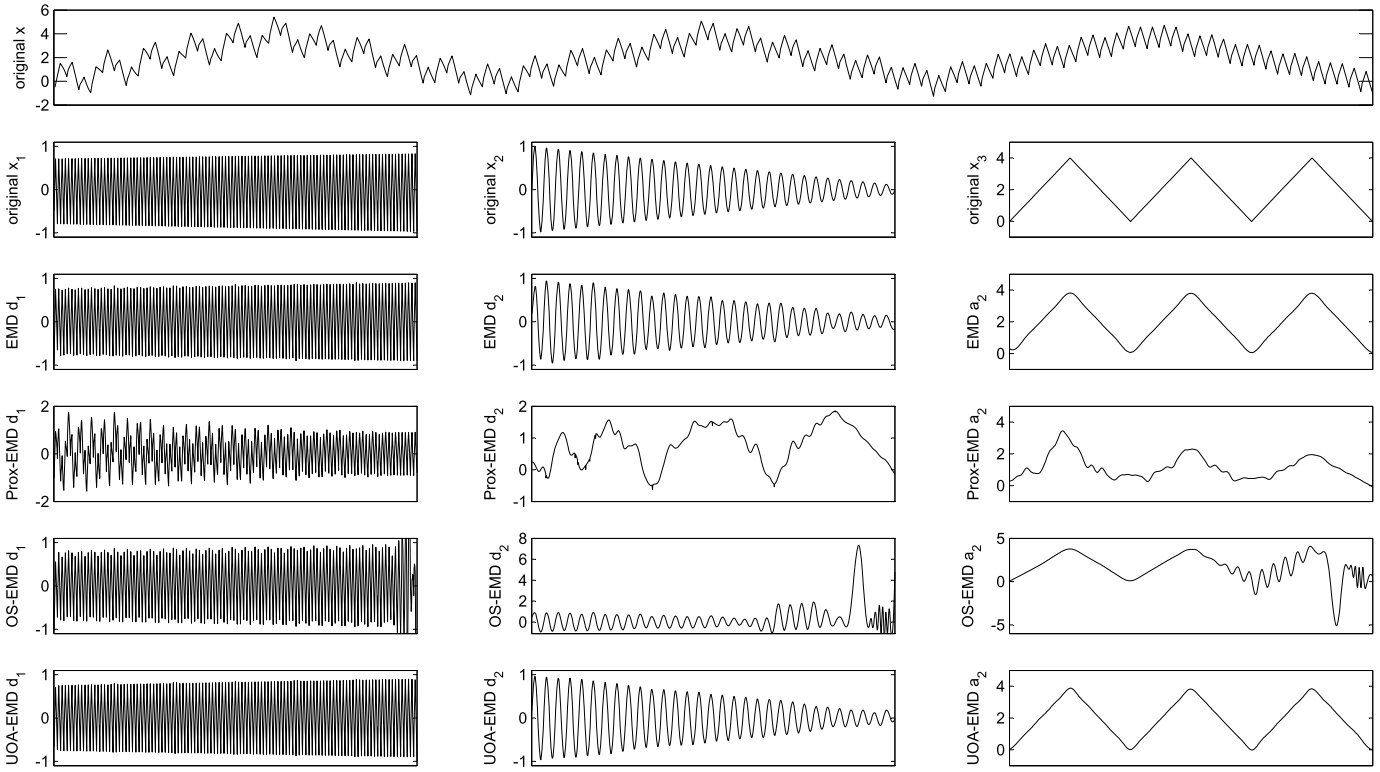

Fig. 3. Sum of two triangular waveforms and an FM sinusoidal signal. The original signal x is on the top row, and its components are on the second row. On the following rows are the components extracted *via* traditional EMD, Prox-EMD, OS-EMD and UOA-EMD respectively.

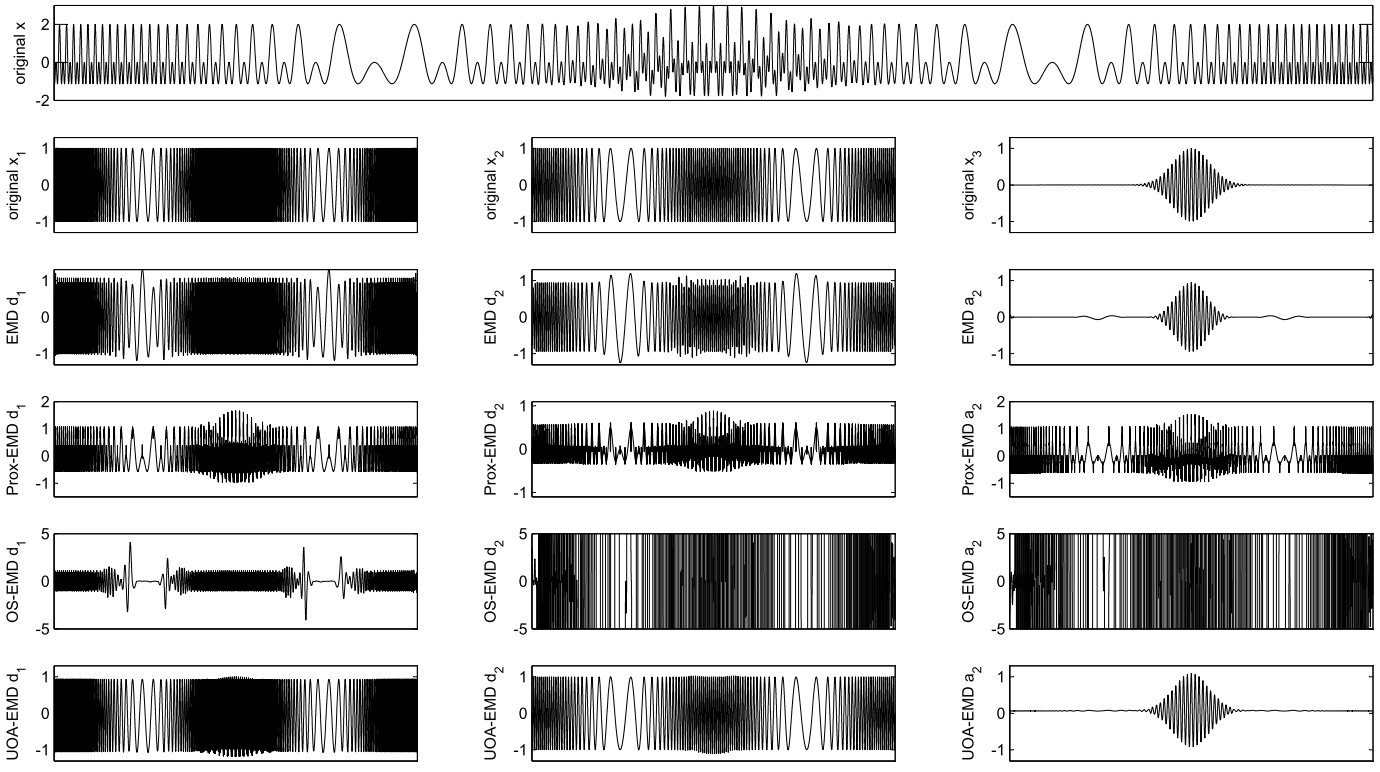

Fig. 4. Sum of two AM–FM signals and a Gaussian atom. The original signal x is on the top row, and its components are on the second row. On the following rows are the components extracted *via* traditional EMD, Prox-EMD, OS-EMD and UOA-EMD respectively.

Table 3
Sum of two AM–FM signals and a Gaussian atom (one million datapoints). Relative square errors and computational times for the four methods.

	Relative square error			Computational time (seconds)
	$x_1(t)$	$x_2(t)$	$x_3(t)$	
EMD	2.04×10^{-2}	2.40×10^{-2}	$\mathbf{5.67 \times 10^{-2}}$	**1.1526**
Prox-EMD	5.20×10^{-1}	6.78×10^{-1}	2.6531	2854
OS-EMD	1.1321*	5.35×10^{8}*	6.05×10^{9}*	711*
UOA-EMD	$\mathbf{8.20 \times 10^{-3}}$	$\mathbf{2.60 \times 10^{-3}}$	1.20×10^{-1}	2.8793

* The algorithm did not accomplished the decomposition and printed an error message.

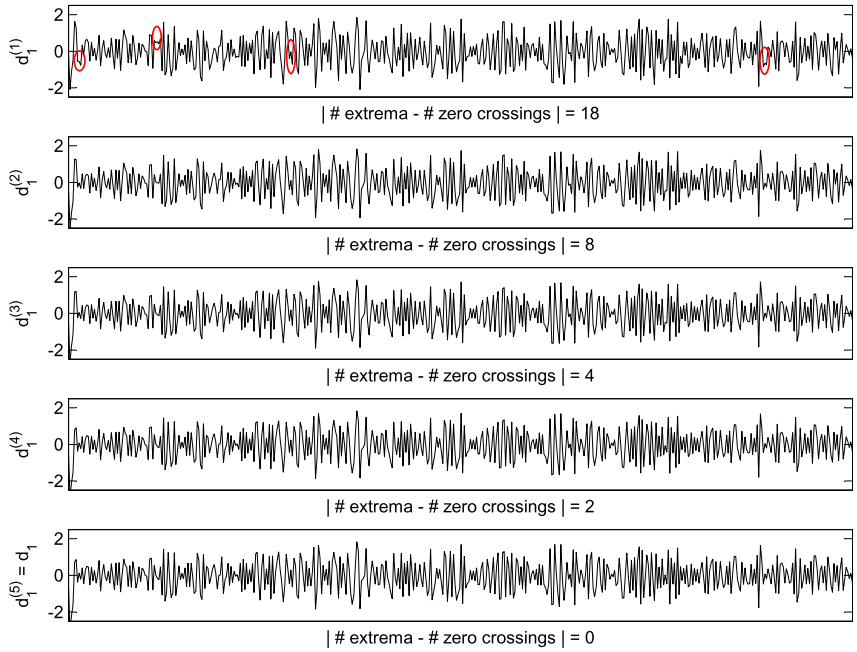

Fig. 5. Sifting process for the first mode of a wGn realization. The most noticeable points where the first mode candidate violates condition (i) are marked with circles. The method here proposed corrects those violations.

5.3. White Gaussian noise and equivalent filter banks

Here we explore an iterative scheme with our method on a 512-sample long white Gaussian noise (wGn) realization with $\mathcal{N} \sim (0, 1)$. We perform sifting iterations until the weak-IMF condition is satisfied (condition (i)) [28]. In Fig. 5 we illustrate the sifting process for the first mode. We used $\lambda = 1$. The most noticeable points where the first mode candidate violates condition (i) are marked with circles; it can be observed that our method corrects those violations at the fifth iteration.

Extensive simulations with wGn were carried out in the past to assess EMD behavior. A quasi-dyadic filter bank structure was revealed when EMD was applied to wGn [12,13,27]. Same feature appears when wGn is analyzed by our method. Following Flandrin et al. [12], we calculated equivalent transfer functions for our method when applied to wGn. Five thousands wGn realizations were decomposed ($\lambda = 1$ and a fixed number of ten sifting iterations) and the average behavior was estimated as in [12]:

$$\hat{S}_k(f) = \sum_{m=-N+1}^{N-1} \hat{r}_k[m]\, w[m]\, e^{-i2\pi f m}, \qquad |f| \leq \frac{1}{2}, \tag{16}$$

with $w[m]$ being a Hamming window, N the mode length, and

$$\hat{r}_k[m] = \frac{1}{J} \sum_{j=1}^{J} \left(\frac{1}{N} \sum_{n=1}^{N-|m|} d_k^j[n]\, d_k^j[n+|m|] \right), \quad |m| \leq N-1 \tag{17}$$

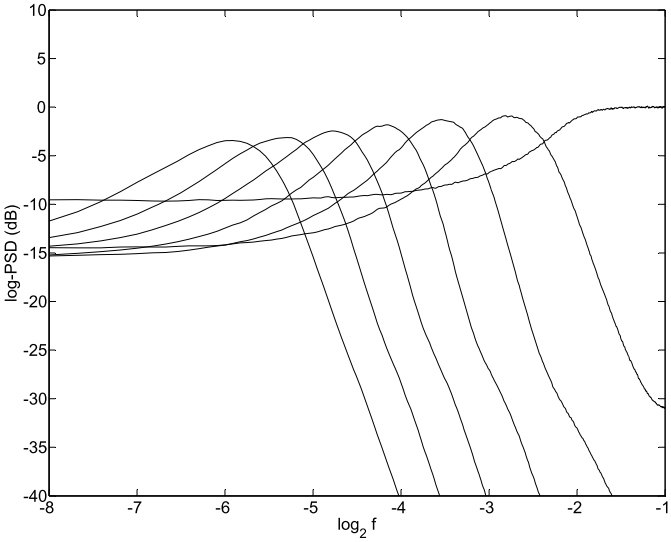

Fig. 6. Equivalent transfer functions $\hat{S}_k(f), 1 \leq k \leq 7$. 5000 wGn realizations were decomposed by our method and the average behavior was estimated according to (16) and (17), following [12].

is the average (over the J realizations) of the empirical estimates of the auto-correlation function where d_k^j is the k-th mode of the j-th wGn realization. Results are depicted in Fig. 6. It can be appreciated that they are very similar to those reported in [12,13].

Self-similarity seems to emerge. In Fig. 7 we plot $\log_2 f_k^*$ vs. k, where $f_k^* = \arg\max_f |\hat{S}_k(f)|$, and a linear fit is superimposed. The slope $\rho = 1.53$ of that fit verifies $f_k^* \propto \rho^{-k}$ and we can state (as in [12,27])

$$\hat{S}_{k'}(f) = \hat{S}_k(\rho^{k'-k} f) \tag{18}$$

for $k' > k \geq 2$. It was shown in [29] that self-similarity coefficient ρ decreases as the number of sifting iterations increases. The relatively low value for ρ obtained in our example (far from the quasi-dyadic case where $\rho \approx 2$ for ten sifting iterations [13,29]) indicates that one sifting iteration of our method is equivalent to several iterations with EMD. This feature was already observed in Section 5.1.

5.4. Local narrow band signals decomposition

In the operator-based approach introduced in [23], the authors mentioned the inability of their method to separate the signal $x(t) = \sin(2t) - \cos(4t)/3$. We present in Fig. 8 the decomposition of such signal by the method here proposed and EMD. We used $\lambda = 1$ and two sifting iterations. Our method achieved RSEs of 1.24×10^{-2} and 1.40×10^{-3} for first and second mode respectively. The RSEs for EMD were: 5.37×10^{-2} and 5.90×10^{-3}.

The authors in [23] also stated that the signal $x(t) = \sin(2t) - (1 + \cos(4t))/4 + \sin(8t) - \cos(16t)/3$ cannot be separated either by their approach nor EMD. For this reason, they proposed a hybrid approach to perform this task. In contrast, our method is able to decompose $x(t)$ by itself, with no further processing. It can be appreciated in Fig. 9 the decomposition results obtained by both EMD and the method here proposed. While our proposal retrieves the four components (except for an irrelevant DC offset in d_3 and a_3), EMD cannot separate the two slowest components in two different modes. Three sifting iterations were needed and, as in the previous examples, we used $\lambda = 1$ (in contrast to [23], where the regularization parameter value needed to be tuned for each single experiment).

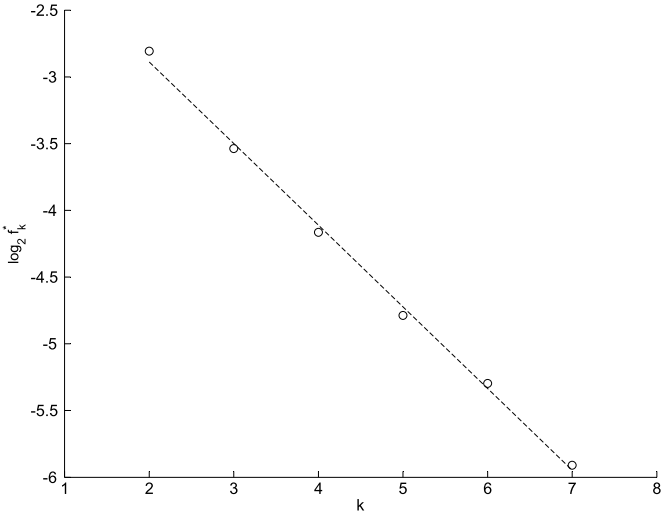

Fig. 7. Positions of equivalent transfer functions maxima. The base 2 logarithm of f_k^* is plotted against mode index k. Linear fit is superimposed and the estimated scaling factor is $\rho = 1.53$.

5.5. Real data

When EMD deals with real data, it frequently experiences mode mixing problems, especially in noisy cases. Although Ensemble EMD (EEMD) [20] alleviates this problem, it creates new ones: the reconstructed signal (i.e. the sum of the modes) includes residual noise and the final averaging is not straightforward since different realizations of signal plus noise may produce different number of modes. The Complete EEMD with Adaptive Noise (CEEMDAN) [25,26] solves this problem by computing a unique first residue (independent from the noise realization) and adding a particular noise at each stage. However, the selection of the optimal parameters (amplitude of added noise and ensemble size) is still an open issue [30], and the ensemble methods cannot guarantee the fulfillment of IMF conditions.

The new method here presented makes no use of added noise, so the exact reconstruction of the signal is not a problem. Also, its sifting iterations appear to be "stronger" (one of them is equivalent to several of EMD's).

To illustrate the advantages of our method in real data, we decompose a voice signal (sustained /a/ vowel). We used $\lambda = 1$, the stopping criterion (9) with $z = 10^{-4}$ (suggested value in [20]) and the number of sifting iterations not fixed but limited to a maximum of 30. Results are presented on left column of Fig. 10. For comparison purposes, we decomposed the same signal also *via* EMD, EEMD and CEEMDAN. We used the same stopping criterion for EMD, with no limit for the sifting iterations. Both noise-assisted methods (EEMD and CEEMDAN) used the same parameters: 0.2 for the amplitude of the added noise [30] and 20 for the ensemble size; and also the same stopping criterion.

When analyzing a quasiperiodic signal as the one studied here, one may expect to extract quasiperiodic components. That is the case for the method here presented. On the first column of Fig. 10, the first two modes seem to extract most of the noise, while modes three to six seem to express most of the signal information. Moreover, the sixth mode captures almost perfectly F_0, the fundamental frequency of the voice signal (inverse of the distance

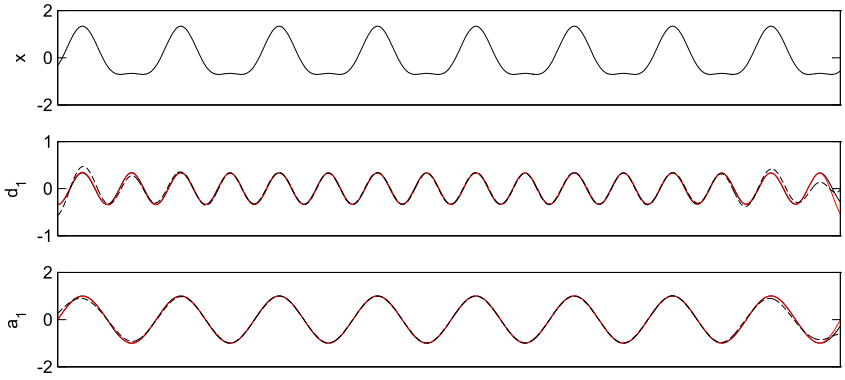

Fig. 8. The signal $x(t) = \sin(2t) - \cos(4t)/3$ is on the top row. In second and third row are original signal components (black solid line), results with our method UOA-EMD (red [gray] solid line), and results with traditional EMD (black dashed line). Signal $x(t)$ cannot be correctly decomposed by the proposal in [23].

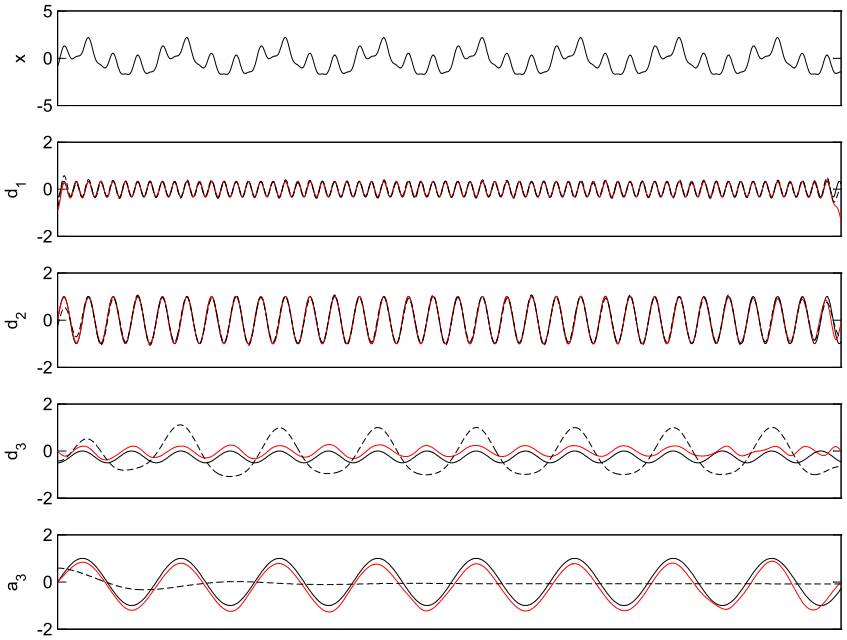

Fig. 9. The signal $x(t) = \sin(2t) - (1 + \cos(4t))/4 + \sin(8t) - \cos(16t)/3$ is on the top row. In second, third, fourth and fifth row are original signal components (black solid line), results with our method UOA-EMD (red [gray] solid line), and results with traditional EMD (black dashed line).

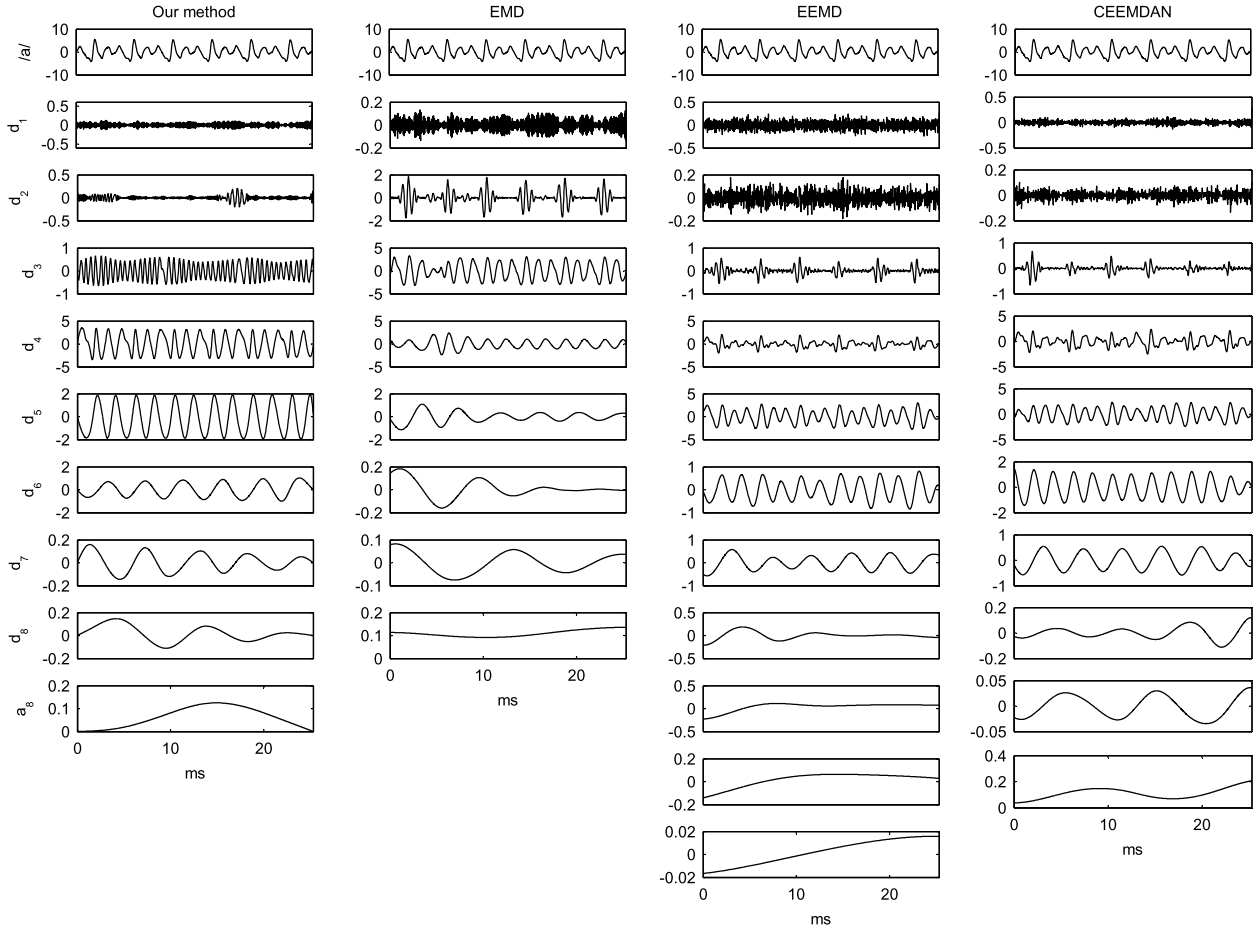

Fig. 10. Decomposition of a voice signal. Our method UOA-EMD seems to achieve the most regular decomposition and sixth mode catches F_0 almost perfectly. EMD is not able to do so. EEMD's seventh mode captures F_0 quite well but misses the final cycle. CEEMDAN's seventh mode captures F_0.

between successive glottal impulses). In contrast, EMD (second column of Fig. 10) presents mode mixing between modes two and three, and between modes three and four. Also, no EMD mode is able to catch F_0. In third column of Fig. 10, EEMD's modes three to seven are quite regular and quasiperiodic, although it can be observed positive minima and negative maxima in the fourth mode, in clear violation to IMF condition (i). Final trend is spread between modes nine to eleven because different realizations produced different number of modes. Besides these problems, the major drawback in this case is the reconstruction error, which is quite large for this ensemble size. CEEMDAN's modes (last column of Fig. 10) are also quite regular, with mode four violating IMF condition (i). The results in this application are in clear favor of the method proposed in the present work.

6. Conclusions

We have proposed an alternative formulation for EMD. Our approach is based on an unconstrained problem, with a unique analytic solution and only one parameter is needed (λ) in the problem statement. An additional benefit for the user, is that the value of λ does not need to be perfectly fit because the results can be refined by sifting, although $\lambda = 1$ seems to be a reasonable choice for most cases. Also, a key element such as matrix P is straightforward to construct. For these reasons our algorithm is simpler than previous approaches. Additionally, the results here presented can be easily reproduced, since analytic solution of the optimization problem has been derived.

The construction of the modes makes our method complete because their sum retrieves the original signal, in contrast to [11] where the reconstruction is not guaranteed. Computational cost is similar to EMD's. For some simulations, the cost was in favor of our method. We must remark that the cost of our proposal is at least two orders of magnitude lower than those of other optimization-based methods (Pustelink et al. and Oberlin et al.).

By making no explicit use of envelopes to find the local mean, the method introduced in this paper avoids possible problems present in the original formulation of EMD, such as overshoot (undershoot), i.e. global maximum (minimum) of the upper (lower) envelope greater (lesser) than global maximum (minima) of the signal [14]. As in traditional EMD, one must avoid to use an extremely large number of sifting iterations, in order to not oversmooth the modes' envelopes.

Summarizing, the new method here presented catches most flavors of the original EMD, with a more solid mathematical framework, which could lead to shed light on analytical properties of EMD. It also works in a wide range of applications where other optimization approaches fail. Additionally, its application to real and simulated signals yields comparable or even better results than traditional EMD.

Acknowledgments

This work was supported by the Argentine National Agency for Scientific and Technological Promotion (ANPCyT-Argentina) under grant PICT-2012 2954, Universidad Nacional de Entre Ríos (Argentina) under grant PID 6136, and the Argentine National Scientific and Technical Research Council (CONICET-Argentina).

References

[1] N.E. Huang, Z. Shen, S.R. Long, M.C. Wu, H.H. Shih, Q. Zheng, N. Yen, C.C. Tung, H.H. Liu, The empirical mode decomposition and the Hilbert spectrum for nonlinear and non-stationary time series analysis, Proc. R. Soc. Lond. A 454 (1998) 903–995.

[2] A. Mert, A. Akan, Detrended fluctuation thresholding for empirical mode decomposition based denoising, Digit. Signal Process. 32 (2014) 48–56.

[3] E. Deléchelle, J. Lemoine, O. Niang, Empirical mode decomposition: an analytical approach for sifting process, IEEE Signal Process. Lett. 12 (11) (2005) 764–767.

[4] Z. Xu, B. Huang, K. Li, An alternative envelope approach for empirical mode decomposition, Digit. Signal Process. 20 (1) (2010) 77–84.

[5] S.D. Hawley, L.E. Atlas, H.J. Chizeck, Some properties of an empirical mode type signal decomposition algorithm, IEEE Signal Process. Lett. 17 (1) (2010) 24–27.

[6] I. Daubechies, J. Lu, H.-T. Wu, Synchrosqueezed wavelet transforms: an empirical mode decomposition-like tool, Appl. Comput. Harmon. Anal. 30 (2) (2011) 243–261, http://dx.doi.org/10.1016/j.acha.2010.08.002.

[7] H. Wu, P. Flandrin, I. Daubechies, One or two frequencies? The synchrosqueezing answers, Adv. Adapt. Data Anal. 3 (1–2) (2011) 29–39.

[8] B. Huang, A. Kunoth, An optimization based empirical mode decomposition scheme, J. Comput. Appl. Math. 240 (2013) 174–183.

[9] T. Oberlin, S. Meignen, V. Perrier, An alternative formulation for the empirical mode decomposition, IEEE Trans. Signal Process. 60 (5) (2012) 2236–2246, http://dx.doi.org/10.1109/TSP.2012.2187202.

[10] N. Pustelnik, P. Borgnat, P. Flandrin, A multicomponent proximal algorithm for empirical mode decomposition, in: 20th European Signal Processing Conference, EUSIPCO 2012, 2012, pp. 1880–1884.

[11] N. Pustelnik, P. Borgnat, P. Flandrin, Empirical mode decomposition revisited by multicomponent non-smooth convex optimization, Signal Process. 102 (2014) 313–331.

[12] P. Flandrin, G. Rilling, P. Gonçalvès, Empirical mode decomposition as a filter bank, IEEE Signal Process. Lett. 11 (2) (2004) 112–114, http://dx.doi.org/10.1109/LSP.2003.821662.

[13] Z. Wu, N.E. Huang, A study of the characteristics of white noise using the empirical mode decomposition method, Proc. R. Soc. Lond. A 460 (2004) 1597–1611.

[14] S. Meignen, V. Perrier, A new formulation for empirical mode decomposition based on constrained optimization, IEEE Signal Process. Lett. 14 (12) (2007) 932–935.

[15] R.C. Aster, B. Borchers, C.H. Thurber, Parameter Estimation and Inverse Problems, 2nd edn., Academic Press, 2012.

[16] J.E. Gentle, Matrix Algebra: Theory, Computations, and Applications in Statistics, Springer, 2010.

[17] G. Rilling, P. Flandrin, One or two frequencies? The empirical mode decomposition answers, IEEE Trans. Signal Process. 56 (2008) 85–95.

[18] G. Rilling, P. Flandrin, Sampling effects on the empirical mode decomposition, Adv. Adapt. Data Anal. 1 (2009) 43–59.

[19] N.E. Huang, M.-L.C. Wu, S.R. Long, S.S. Shen, W. Qu, P. Gloersen, K.L. Fan, A confidence limit for the empirical mode decomposition and Hilbert spectral analysis, Proc. R. Soc. Lond. A 459 (2037) (2003) 2317–2345.

[20] Z. Wu, N.E. Huang, Ensemble empirical mode decomposition: a noise-assisted data analysis method, Adv. Adapt. Data Anal. 1 (1) (2009) 1–41.

[21] G. Rilling, P. Flandrin, P. Gonçalvès, On empirical mode decomposition and its algorithms, in: Proc. IEEE-EURASIP Workshop NSIP-03, Grado, Italia, 2003.

[22] H. Hong, X. Wang, Z. Tao, Local integral mean-based sifting for empirical mode decomposition, IEEE Signal Process. Lett. 16 (10) (2009) 841–844.

[23] S. Peng, W. Hwang, Adaptive signal decomposition based on local narrow band signals, IEEE Trans. Signal Process. 56 (7) (2008) 2669–2676.

[24] S. Peng, W.-L. Hwang, Null space pursuit: an operator-based approach to adaptive signal separation, IEEE Trans. Signal Process. 58 (5) (2010) 2475–2483.

[25] M.A. Colominas, G. Schlotthauer, M.E. Torres, Improved complete ensemble EMD: a suitable tool for biomedical signal processing, Biomed. Signal Process. Control 14 (2014) 19–29.

[26] M.E. Torres, M.A. Colominas, G. Schlotthauer, P. Flandrin, A complete ensemble empirical mode decomposition with adaptive noise, in: Proc. of the 36th Int. Conf. on Acoustics, Speech and Signal Processing, ICASSP 2011, Prague, Czech Republic, 2011, pp. 4144–4147.

[27] P. Flandrin, P. Gonçalvès, Empirical mode decomposition as a data-driven wavelet-like expansion, Int. J. Wavelets Multiresolut. Inf. Process. 2 (4) (2004) 1–20.

[28] R.C. Sharpley, V. Vatchev, Analysis of the intrinsic mode functions, Constr. Approx. 24 (2006) 17–47, http://dx.doi.org/10.1007/s00365-005-0603-z.

[29] G. Rilling, Décompositions modales empiriques-contributions à la théorie, l'algorithmie et l'analyse de performances, Ph.D. thesis, École Normale Superiéure de Lyon, France, 2007.

[30] M.A. Colominas, G. Schlotthauer, M.E. Torres, P. Flandrin, Noise-assisted methods in action, Adv. Adapt. Data Anal. 04 (04) (2012) 1250025, http://dx.doi.org/10.1142/S1793536912500252.

Marcelo A. Colominas was born in Resistencia, Argentina, in 1985. He received the Bioengineer's degree from Universidad Nacional de Entre Ríos in 2011. He is currently working towards the Ph.D. degree in the Signals and Nonlinear Dynamics Laboratory (SNDL), Universidad Nacional de Entre Ríos, and the National Scientific and Technical Research Council (CONICET), Argentina. His research interests are biomedical signal processing and data-driven methods.

Gastón Schlotthauer was born in Galarza, Argentina, in 1974. He received the Bioengineering and M.Sc. in Biomedical Engineering degrees from Universidad Nacional de Entre Ríos (UNER), Argentina, in 2000 and 2007 respectively, and the Ph.D. in Engineering from Universidad Nacional del Litoral (UNL), Argentina, in 2010. He joined the Signals and Nonlinear Dynamics Laboratory (SNDL) and the Department of Mathematics at Faculty of Engineering (UNER) in 1996 and 1998 respectively, and became an Assistant Professor in 2003. Since 2011 he is a Research Scientist at the National Scientific and Technical Research Council (CONICET). His research interests include biomedical signal processing, adaptive signal processing, nonlinear dynamics, and pattern recognition.

María E. Torres was born in Rosario (Santa Fe), Argentina. She received the degree in Mathematics (Hons.) in 1975 and the Ph.D. Math degree in 1999, both from the Universidad Nacional de Rosario (UNR), Argentina. In 1976 she joined the Universidad Nacional del Litoral (UNL), Argentina, and the UNR as Graduate Teaching Assistant and as Assistant Professor. Since 1985 she is with the Universidad Nacional de Entre Ríos (UNER) and holds a Professor position at the Math and Informatics Department. Since 1994 she is Research Director of the Signals and Nonlinear Dynamics Laboratory (SNDL). She held different executive positions in UNER: Director of the Postgraduates Program in Biomedical Engineering, Director of the Math Department, Member of the University Directive Council in the Research Committee. Since 2007 she is also professor at the Universidad Nacional del Litoral. Since 2008 she is with the National Scientific and Technical Research Council (CONICET). Dr. Torres received paper awards in several Argentine and international congresses. Her research interests include biomedical signal processing, wavelets, adaptive signal processing, nonlinear dynamics, fractal and multifractal analysis, and pattern recognition.